Global Soil Moisture Estimation at High Resolution:
A Microwave-Optical/IR Synergistic Approach

Narinder S. Chauhan*
NPOESS Integrated Program Office, Silver Spring, MD 20910

Shawn Miller and Phillip Ardanuy
Raytheon ITSS, Lanham MD 20706

ABSTRACT: An approach is evaluated for the estimation of soil moisture at high resolution using satellite microwave and optical/infrared (IR) data. This approach can be applied to data acquired by the Visible/Infrared Imager Radiometer Sensor Suite (VIIRS) and a Conical Scanning Microwave Imager/Sounder (CMIS), planned for launch in 2007-2010 time frame under the National Polar-Orbiting Operational Environmental Satellite System (NPOESS). The approach for soil moisture estimation involves two steps. In the first step, a passive microwave remote sensing technique is employed to estimate soil moisture at low resolution (~25km). This involves use of a simplified radiative transfer model to invert dual-polarized microwave brightness temperature. In the second step, the microwave-derived low-resolution soil moisture is linked to the scene optical/IR parameters, such as; Normalized Difference Vegetation Index (NDVI), surface albedo, and Land Surface Temperature (LST). The linking is based on 'Universal Triangle' approach of relating land surface parameters to soil moisture. The optical/IR parameters are available at high-resolution (~1km) but are aggregated to the microwave resolution for the purpose of building the linkage model. The linkage model in conjunction with high-resolution NDVI, surface albedo, and LST is then used to disaggregate microwave soil moisture into high-resolution soil moisture.

The technique is applied to data from the Special Sensor Microwave Imager (SSM/I) and Advanced Very High Resolution Radiometer (AVHRR) acquired for the Southern Great Plains (SGP-97) experiment conducted in Oklahoma in June-July, 1997. An error budget analysis performed on the estimation procedure shows that the root mean square (RMS) error in the estimation of soil moisture is of the order of 5 percent. Predicted soil moisture results at high resolution agree reasonably well with low resolution results in both magnitude and spatio-temporal patterns. The high-resolution results are also compared with in-situ (0-5cm deep) point measurements. While the trends are similar, the soil moisture estimates in the two cases are different. Issues involving comparison of satellite derived soil moisture with in situ point measurements are also discussed.

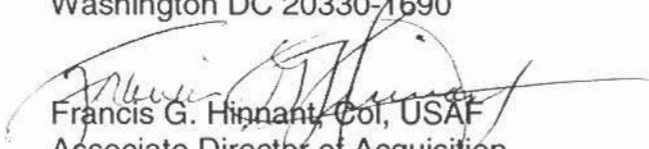* The author is affiliated with The Aerospace Corporation

DEPARTMENT OF THE AIR FORCE
HEADQUARTERS UNITED STATES AIR FORCE

APR 2 3 2001

MEMORANDUM FOR: SAF/PAS
1690 Air Force Pentagon - 5D227
Washington DC 20330-1690

FROM: Francis G. Hinnant, Col, USAF
Associate Director of Acquisition
NPOESS Integrated Program Office
8455 Colesville Rd, Suite 1450
Silver Spring, MD 20910

SUBJECT: Soil Moisture Approach and Algorithm

Enclosed are the required ten (10) copies of the subject paper. This paper, authored by Narinder Chauhan, will be submitted to the International Journal of Remote Sensing for publication.

The program office has reviewed the science information and found it appropriate for public disclosure without change. A response is requested not later than 18 May 01.

Point of contact on this matter is Maj Elisa Kang, NPOESS IPO/ADA at 301-427-2084 (Ext. 142).

cc: ADA (E. Kang)

Attachment: Paper—10 copies

Global Soil Moisture Estimation at High Resolution:
A Microwave-Optical/IR Synergistic Approach

Narinder S. Chauhan*
NPOESS Integrated Program Office, Silver Spring, MD 20910

Shawn Miller and Phillip Ardanuy
Raytheon ITSS, Lanham MD 20706

ABSTRACT: An approach is evaluated for the estimation of soil moisture at high resolution using satellite microwave and optical/infrared (IR) data. This approach can be applied to data acquired by the Visible/Infrared Imager Radiometer Sensor Suite (VIIRS) and a Conical Scanning Microwave Imager/Sounder (CMIS), planned for launch in 2007-2010 time frame under the National Polar-Orbiting Operational Environmental Satellite System (NPOESS). The approach for soil moisture estimation involves two steps. In the first step, a passive microwave remote sensing technique is employed to estimate soil moisture at low resolution (~25km). This involves use of a simplified radiative transfer model to invert dual-polarized microwave brightness temperature. In the second step, the microwave-derived low-resolution soil moisture is linked to the scene optical/IR parameters, such as; Normalized Difference Vegetation Index (NDVI), surface albedo, and Land Surface Temperature (LST). The linking is based on 'Universal Triangle' approach of relating land surface parameters to soil moisture. The optical/IR parameters are available at high-resolution (~1km) but are aggregated to the microwave resolution for the purpose of building the linkage model. The linkage model in conjunction with high-resolution NDVI, surface albedo, and LST is then used to disaggregate microwave soil moisture into high-resolution soil moisture.

The technique is applied to data from the Special Sensor Microwave Imager (SSM/I) and Advanced Very High Resolution Radiometer (AVHRR) acquired for the Southern Great Plains (SGP-97) experiment conducted in Oklahoma in June-July, 1997. An error budget analysis performed on the estimation procedure shows that the root mean square (RMS) error in the estimation of soil moisture is of the order of 5 percent. Predicted soil moisture results at high resolution agree reasonably well with low resolution results in both magnitude and spatio-temporal patterns. The high-resolution results are also compared with in-situ (0-5cm deep) point measurements. While the trends are similar, the soil moisture estimates in the two cases are different. Issues involving comparison of satellite derived soil moisture with in situ point measurements are also discussed.

---

* The author is affiliated with The Aerospace Corporation

I.   INTRODUCTION

As a part of Integrated Program Office (IPO) program, NPOESS will provide an enduring capability to measure atmospheric, land, and ocean environmental parameters on a global basis. The system will provide timely, accurate weather and environmental data to weather forecasters, military, civilian leaders, and the scientific community. NPOESS converges the National Oceanic and Atmospheric Administration's (NOAA) Polar Operational Environmental Satellites (POES) and the Defense Department's Defense Meteorological Satellite Program (DMSP) into a single system. NPOESS will operate in near circular, sun-synchronous orbit and is scheduled to fly in the 2007-2010 time frame. A host of satellites with sensors operating in different frequency regions of the electromagnetic spectrum will have equatorial node crossings at 0530, 0930 and 1330 local times. The VIIRS and CMIS will form an important part of NPOESS and will share the same platform. The VIIRS and CMIS will be successors in technology to AVHRR and SSM/I, respectively. There are about five dozens of parameters to be retrieved from the remote sensing data collected by NPOESS and among them six are declared as 'key' parameters (NPOESS, 1999). The 'key' parameters are particularly important to NPOESS mission and soil moisture is one of the 'key' parameters. In this paper, we describe a synergistic optical/IR and microwave approach that is being developed for NPOESS for estimating soil moisture at a kilometer resolution.

Recent studies have shown the effects of soil moisture on the feedbacks between land-surface and atmospheric processes that lead to climate irregularities (Brubaker and Entekhabi, 1996; Delworth and Manabe, 1989). Simulations with Global Climate Models (GCM) have shown that improved characterizations of surface soil moisture and other land surface parameters in numerical weather prediction models can lead to both weather and climate forecast improvement (Beljaars et al., 1996). Soil moisture is also an important component in the terrestrial ecosystem processes. It provides a link between the terrestrial surface and the atmosphere through its effects on surface energy and soil moisture fluxes (Sellers et al., 1986). Thus, the ability to determine the spatial and temporal distribution of soil moisture would be of significant help in understanding the Earth as an integrated system. Additionally, the timely information of soil moisture is also used by the military for the accurate planning of infantry and vehicular traffic in the remote areas. NPOESS will provide such a capability on an operational and continuous basis.

Currently, soil moisture data product is not available globally from any of the spaceborn missions. A few surrogates of soil moisture such as soil wetness, flood index, crop index, Antecedent Precipitation Index (API), etc. are however available. These surrogates are insufficient substitutes of soil moisture estimates and provide crude and qualitative information about the soil moisture. Both microwave and optical/IR remote sensing techniques are capable of sensing soil moisture, but the implementation of these sensing techniques from space platform for global soil moisture estimation has been lacking. Microwave remote sensing has the potential to provide a direct measure of soil moisture. It also has the advantage of all-weather observations and penetration into vegetation

canopy for the soil moisture sensing. However, there are many reasons as to why microwave techniques have not been applied for the global estimation of soil moisture. First, the spatial resolution of passive microwave sensors from space is poor, second, the current satellite channels do not provide adequate soil moisture sensitivity for majority of vegetation covers and the third, the 'a priori' information required in the existing soil moisture estimation algorithms can not be obtained globally. In controlled experiments, longer wavelengths (e.g. L-band) have been used since they provide adequate sensitivity to soil moisture under most vegetation covers. However, longer wavelengths require large antennas in orbit and large rotating antennas in orbit are an engineering challenge and the solutions are expensive. The problem scales inversely with frequency and that is why an imaging radiometer at L-band has not been flown in space. In fact, the resolution available for passive microwave remote sensing from space has improved very little from its beginnings with the launch of the Electronically Scanned Microwave Radiometer (ESMR) in 1972. Consequently, despite the success of microwave remote sensing of soil moisture in controlled environments, few efforts have been made to extend soil moisture remote sensing to global scale. Presently, neither the microwave sensor technology is able to provide high-resolution data nor the microwave algorithms employing *solely* microwave data are robust enough to estimate soil moisture without 'a priori' information.

(In this paper, the terms low resolution, microwave resolution, 25-km resolution are used interchangeably. Similarly, the terms high resolution, optical resolution, 1-km resolution are also used interchangeably).

II.   HISTORICAL PERSPECTIVE

A number of techniques spanning across the whole electromagnetic spectrum have been used to sense soil moisture. However, techniques in the optical/IR and microwave frequency regimes have attracted more attention. The surface radiant temperature of bare soil illuminated by sunlight is highly correlated with soil wetness (see e.g. Idso et al., 1975). The spatial variations of the radiant temperature are strongly dependent on the fraction of the bare soil viewed by the radiometer and surface soil water contents. Vegetation, however, complicates the relationship. A rigorous way to implore this relationship is through the modeling of the Soil Vegetation Atmosphere Transfer (SVAT) of energy using an energy budget approach. However, Carlson et al. (1994) and Gillies et al. (1997) were able to generate regression relations among NDVI, soil moisture, and soil temperature by careful analyses of available data. These results were reaffirmed by the University of Pennsylvania SVAT model (Carlson et al., 1995). A unique relationship between surface soil moisture availability and radiant temperature does not exist in the presence of vegetation cover, but the relative variations in NDVI and temperature show a fairly stable relationship to soil moisture availability over a wide range of climatic conditions and land surface types (Carlson et al., 1994).

Optical/IR sensing techniques also provide a good spatial resolution and efforts were made in seventies to use them for soil moisture estimation (Idso et al., 1975; Idso et al., 1976; Price, 1977). However, the returns from optical/IR sensors are equally sensitive to

3

the soil types and it is difficult to decouple the two signatures. In addition, the soil moisture estimates derived from optical/IR sensors require surface micrometeorological and atmospheric information that is not routinely available. Controlled experiments continue to show that the optical/IR approach has the potential to sense soil moisture, but the implementation particularly from space, has not been accomplished so far. Fresh attempts such as those by Cracknell and Xue (1996) are underway for the determination of thermal inertia from space. A soil moisture product has not been slated for the future optical/IR missions so far.

Passive microwave remote sensing has been widely used to provide a quantitative, direct estimate of soil moisture (Njoku and Li, 1999; Jackson et al., 1982; Engman, 1991). The soil moisture maps obtained in Southern Great Plains experiment (SGP-97), Washita-92, Moonsoon-90 and First ISLSCP Field Experiment (FIFE) were all provided by passive sensors operating at L-band. In most cases, a simplified radiative transfer model is inverted to obtain Fresnel reflectivity. 'A priori' information of vegetation optical depth and root mean square (RMS) height of the soil surface, is required to estimate soil moisture (O'Neill et al., 1996). However, the channel frequencies and the spatial resolution of the current generations of spaceborn microwave radiometers are not optimal for land remote sensing. SSM/I launched in 1987 has the lowest frequency of 19.4 GHz and a spatial resolution of ~56 km. The Scanning Multichannel Microwave Radiometer (SMMR) launched on the Nimbus-7 satellite in 1978, had a spatial resolution of ~150 km at its lowest frequency of 6.6 GHz. Lower frequencies such as L-band are preferred for soil moisture since they provide better sensitivity to soil moisture for the vegetation cover. But, because of practical problems of supporting a large size low-frequency antenna in space, the prospectus of having a spaceborn low-frequency microwave sensor, remains uncertain.

A few attempts have been made to use microwave satellite data for the soil moisture estimation. Van de Griend and Owe (1993) and Owe et al. (1992) have written series of paper on the characterization of soil moisture and vegetation properties from SMMR data over Southern Africa. Jackson (1997) used SSM/I data at 19.4 GHz together with 'a priori' values of single scattering albedo and optical depth, to estimate soil moisture for a grass-dominated subhumid area near Oklahoma . In a recent paper, Njoku and Li (1999) have demonstrated an estimation approach that can be used to derive soil moisture from Advanced Microwave Scanning Radiometer (AMSR) scheduled to fly on Earth Observing System (EOS) PM platform in 2001. The lowest frequency on AMSR will be 6.9 GHz and the footprint size of 43km x 75km. The microwave equivalent of thermal inertia, known as radiobrightness thermal inertia, has also been used to estimate soil moisture from satellite microwave data for the controlled experiments (England et al., 1992). None of the above techniques address the problem of poor resolution of the microwave radiometers.

III. METHOD

To achieve accuracy and high spatial resolution, it seems natural to have a technique that combines the strengths of microwave as well as optical/IR remote sensing approaches for

4

the soil moisture estimation. This paper describes a two-step approach to obtain operational, reasonably accurate, high-resolution soil moisture by linking microwave-derived soil moisture estimates with optical/IR parameters. First, the soil moisture at low resolution is retrieved from microwave data. This is achieved by inverting the ratio of horizontal to vertical Fresnel reflectivities. The technique is suitable for satellite remote sensing and does not require 'a priori' information. The second step involves relating the microwave-derived soil moisture to NDVI, temperature and albedo. This is done through regression following the Carlson's work (http://www.essc.psu.edu/~tnc/). These regression relations, in conjunction with high resolution NDVI, LST, and albedo are then regressed backward to obtain soil moisture at high resolution. The enhancement of spatial resolution of soil moisture from ~25 km to ~1 km, is an important development with wide applications.

The flowchart diagram of the soil moisture estimation algorithm is given in Figure 1, and details of the above steps are described in the following sections.

This soil moisture estimation technique is later applied to data from SSMI and AVHRR over the SGP-97 experimental region, near Oklahoma (Section IV). In-situ soil moisture (0-5 cm deep) collected during the SGP-97 experiment is compared against the predictions. An error and sensitivity analysis has also been performed on the estimation procedure (Section V). For the microwave part, error analysis is carried out using an emission model that is robust and has been validated for a variety of canopy covers. For the high-resolution estimation part, error analysis is performed using SSM/I and AVHRR data. Finally, the limitations of point measurements for validation of satellite soil moisture are also discussed.

A. Soil Moisture at Low Resolution (Microwave Estimation of Soil Moisture)
Microwave radiometer response (Chauhan et al. 1994) computed by the forward model (Appendix A) is inverted for the determination of soil moisture. The full-scale model is too complicated to be inverted. It is simplified for weak vegetation cover under the assumption that the vegetation scattering is negligibly small. In addition, it is assumed that the scattering from the rough ground surface is also negligibly small. Therefore, the brightness temperature T_q of a vegetated and/or a rough surface is written as

$$T_q = T \left\{ 1 - |R_q|^2 e^{-2\tau_q} e^{-4k_o^2 s^2 \cos^2 \theta} \right\} \tag{1}$$

where $|R_q|^2$ denotes the Fresnel reflectivity of the flat surface and is a measure of soil moisture. In above equation, τ_q, k_o, s, θ are vegetation optical depth, free-space propagation constant, rms height of the rough surface, and view angle respectively. The suffix q denotes polarization and can be either h (horizontal) or v (vertical) and T is the physical temperature of the scene. If data from both horizontal and vertical polarizations is used, then Eq. (1) can be rewritten as (Chauhan, 2001),

5

$$\left\{\frac{T-T_h}{T-T_v}\right\} = \left|\frac{R_h}{R_v}\right|^2 e^{2(\tau_v - \tau_h)} \qquad (2)$$

The suffix h and v refers to horizontal and vertical polarization respectively. It is noticed that Eq. (2) is independent of root mean square roughness height (s) and depend only on the difference between the vegetation optical depths at like polarizations i.e. $(\tau_v - \tau_h)$.

Therefore, if T_h, T_v, T, $(\tau_v - \tau_h)$ are known, then $\left|\dfrac{R_h}{R_v}\right|^2$ can be calculated from Eq. (2) which can be converted to yield soil moisture. An examination of canopy data suggests that scatterers in weaker vegetation do not have any dominant angular orientations. Consequently, horizontal and vertical optical depth gets closer to one another. In the work by van de Griend and Owe (1993) on soil moisture from Savanna types of vegetation, it is assumed that $\tau_h - \tau_v \cong 0$ for the SSM/I data at 19.4 GHz and 37 GHz. Therefore, assuming that $\tau_h - \tau_v \cong 0$ for weak vegetation, Eq. (2) is further simplified to

$$\left\{\frac{T-T_h}{T-T_v}\right\} = \left|\frac{R_h}{R_v}\right|^2 \qquad (3)$$

Since microwave brightness temperature and the physical temperature can be measured directly by remote sensing, $\dfrac{R_h}{R_v}$ can be calculated from Eq. (3) without any 'a priori' information about the canopy or the ground. The reflection coefficients in Eq. (3) are expressed in analytical form as

$$R_h = \frac{\cos\theta - \sqrt{\varepsilon_g - \sin^2\theta}}{\cos\theta - \sqrt{\varepsilon_g + \sin^2\theta}} \qquad (4)$$

$$R_v = \frac{\varepsilon_g \cos\theta - \sqrt{\varepsilon_g - \sin^2\theta}}{\varepsilon_g \cos\theta - \sqrt{\varepsilon_g + \sin^2\theta}} \qquad (5)$$

In above equations ε_g is the real part of soil dielectric constant. The imaginary part of ε_g is small and therefore ignored (Chauhan, 1997) for the soil moisture retrievals. After doing a little bit of algebra, ε_g can be expressed from Eqs. (4) and (5) as a function of $\dfrac{R_h}{R_v}$ (Chauhan 2001). Finally, the volumetric soil moisture is obtained from ε_g by using the empirical relationship given by Hallikainen et al. (1985).

The microwave frequencies from satellites have limited capability to penetrate vegetation. Consequently, the application of microwave algorithm to 19.4 GHz data from SSM/I will be limited to vegetation having NDVI less than or equal to 0.4. Based on the

6

work of Myneni et al. (1997), NDVI of 0.4 translates to LAI of 1-2 for most biomes (Figure 5a in Myneni et al. [1997]). The limit on NDVI will change if lower microwave frequencies such as C or L-band are available for satellite remote sensing. The dual-polarization technique described here is particularly useful for global soil moisture estimation because the technique can operate without the global estimates of ground and vegetation information.

B. Soil Moisture at High Resolution
Soil moisture coupling to land-surface interactions has been used in the past to quantify soil moisture signatures (Carlson et al., 1994; Nemani et al., 1993). NDVI and soil temperature are proven indicators of the vegetative and thermal potential of the land surface. However, the vegetation and soil temperature have a complicated dependence on soil moisture. Careful analyses of data by Carlson et al., (1994) and Gillies et al., (1997) have shown that there can be a unique relationship among soil moisture, NDVI, and soil temperature for a given region. The results were validated using data analyzed from three experiments conducted at Mahantango, Kansas and in Costa Rica (Carlson et al., 1994). In addition, such relationships are also confirmed by theoretical studies using a soil-vegetation-atmosphere-transfer (SVAT) model.

Figure 2 represents a schematic description of the relationship, sometimes referred to as the 'universal triangle'. Here, soil moisture varies from right (low value) to left (high value) in the triangle. The abscissa and the ordinate are appropriately scaled versions of temperature and NDVI respectively such that

$$T^* = \frac{T - T_o}{T_s - T_o} \tag{6}$$

$$NDVI^* = \frac{NDVI - NDVI_o}{NDVI_s - NDVI_o} \tag{7}$$

where T and NDVI are observed soil temperature and NDVI respectively, and the subscripts o and s stand for minimum and maximum values. Carlson et al. (1994) found that the relationship between soil moisture M, $NDVI^*$, and T^* can be expressed through a regression formula such as

$$M = \sum_{i=0}^{i=n} \sum_{j=0}^{j=n} a_{i,j} NDVI^{*(i)} T^{*(j)} \tag{8}$$

Carlson (1998) argued that a single polynomial such as the one above represents a wide range of surface climate conditions and land surface types. The second or third order polynomial gives a reasonable representation of the data.

To apply Carlson's concept of 'universal triangle' in the present context, the left-hand side in Eq. (8) is replaced by microwave-derived soil moisture. In addition to NDVI and T on the right-hand side of Eq. (8), surface albedo (A) is added to strengthen the

relationship between the high end of soil moisture and measurable land parameters. Therefore, Eq. (8) is modified to:

$$M = \sum_{i=0}^{i=n}\sum_{j=0}^{j=n}\sum_{k=0}^{k=n} a_{ijk} NDVI^{*(i)} T^{*(j)} A^{*(k)}$$

(9)

where

$$A^* = \frac{A - A_o}{A_x - A_o}$$

Expanding Eq. (9) to get a second order polynomial, one obtain

$$\begin{aligned}
M = &\, a_{000} + a_{001}A^* + a_{010}T^* + a_{100}NDVI^* \\
&+ a_{002}A^{*2} + a_{020}T^{*2} + a_{200}NDVI^{*2} \\
&+ a_{011}T^*A^* + a_{101}NDVI^*A^* + a_{110}NDVI^*T^*
\end{aligned}$$

(10)

In the above expansion, the third order terms have been ignored. We have employed Eq. (10) for most of the analysis presented in this paper.

IV.   APPLICATION TO SSM/I AND AVHRR DATA

A. Soil Moisture Mapping

The soil moisture algorithm is applied to data over a mid-west region of United States ($33°N$ to $38°N$, $-100°W$ to $-96°W$) covering the Southern Great Plain (SGP) experiment region. This experiment was conducted in June-July of 1997 and was designed to measure, estimate spatial and temporal variation in soil moisture and other hydrologic variables. The bulk of this region is grassland along with short vegetation in the agricultural fields. Complete details of the experiment and data can be found at http://hydrolab.arsusda.gov/SGP-97.

For the present analysis, satellite data from AVHRR and SSM/I (frequency=19.4 GHz) over the SGP-97 experiment region were acquired for four relatively cloud free days. SSM/I data are at 25-km resolution on cylindrical equal area projection true at 30N and 30S, and AVHRR data are Level 1B with resolution of about 1-km. The LST, NDVI and surface albedo are calculated from AVHRR, Level 1B data that has a resolution close to 1-km. A simple split window method (Price, 1984) employing data from Channel 4 and 5 of AVHRR is used for this purpose. Similarly, surface albedo is calculated by scaling data from Channel 4 and 5 of AVHRR. Both the LST and NDVI are aggregated to a scale of 25-km resolution for their use in the microwave algorithm. Dual polarization method discussed earlier in Section IIIA is applied to brightness temperature (from SSM/I) and aggregated LST to compute soil moisture at 25-km resolution. Since the microwave algorithm is valid for lightly vegetated area, we have limited its application to vegetation covers with NDVI of 0.4. For cloudy pixels, we have used a simplified cloud mask that involves masking cloud pixels based on the visible channel of AVHRR. A new cloud mask for the NPOESS is being developed and will be incorporated in later studies.

8

Figure 3 shows 25-km resolution soil moisture maps for the SGP-97 region for June 29, June 30, July 1, July 2 of 1997. The spatial variations in soil moisture are clearly seen in all the four days. The temporal variations are less prominent and will be discussed in more details in the next section. The eastern part in the SSM/I derived soil moisture image on June 30, July 1-2 is shaded gray because of non-availability of SSM/I data. Generally, the grey/black regions in the map are the areas where soil moisture is not computed. There can be variety of reasons for this; such as high NDVI, corrupted data because of clouds, corrupted data from SSM/I, etc. It is noticed that soil moisture in Fig. 3 exhibits a dry-to-moderate level of moisture with individual pixel values ranging from 5 to 15 percent of volumetric soil moisture. Note that the soil moisture shown in these maps represents the moisture from a very thin soil layer because the sensing frequency is 19.4 GHz. The soil moisture information is also depicted differently in Fig. 4 where soil moisture values of individual pixels are plotted for four days.

To estimate soil moisture at 1-km resolution, first a system of linear equations is set up between SSM/I-derived soil moisture and aggregated NDVI, aggregated albedo, aggregated LST (Eqs. 9,10) for all the pixels in the SGP-97 region. The system is solved and the regression coefficients a_{ijk} (Eq. 9) for the SGP-97 region are determined. To check the accuracy of the regression coefficients, the parameters NDVI, albedo, T are used in conjunction with calculated a_{ijk} in Eq. (9) to compute soil moisture.The RMS error between the regression-derived soil moisture and the SSM/I-derived soil moisture is calculated. In the present case this RMS error is quite small ~ 0.016 for all days. The soil moisture values at 1-km are then obtained by substituting 1-km scale NDVI, albedo, and LST in the right-hand side of Eq. (10) alongwith regression coefficient a_{ijk} calculated earlier. Figure 5 shows 1-km resolution soil moisture maps for the SGP-97 region for June 29, June 30, July 1, July 2 of 1997. A visual inspection of images shown in Figs. 3 and 5 shows that there is a close resemblance between the soil moisture spatial patterns and the quantitative estimates. Clearly, the 1-km soil moisture image shows much more details than the 25-km soil moisture image. The patches of no data in the northern part on June 29 are due to the cloud mask applied to AVHRR data. For comparison sake, 1-km scale soil moisture for individual pixels are been plotted in Fig. 6. The mean and spread of 1-km soil moisture values (Fig. 6) compares closely to that of 25-km soil moisture values (Fig. 4).

B. Comparison with in-situ Measurements
Validation of soil moisture estimation results is difficult and particularly so if satellite data is involved. The difficulty arises not only in the estimation process but also in the measurements of in-situ soil moisture. Several issues are involved in soil moisture measurements. Microwave sensors measure soil moisture in the topmost soil layer (1/10 to 1/4 of a wavelength). At 19 GHz, this layer can be about 0.1-0.4 cm deep. The penetration of microwave signal depends on soil moisture itself. In view of this, it is difficult to decide the depth of soil samples for the in-situ measurements. Soil moisture also changes very rapidly in the topmost soil layer. In addition, there are practical problems in collecting soil samples that are only 0.1-0.4 cm deep. Still further the spatial

distribution of soil moisture depends on soil parameters which are not distributed homogeneously in the area. As a result, the average soil moisture computed from point measurements within a footprint does not give an accurate representation of the soil moisture in the footprint. In view of these uncertainties, a definite conclusion can not be drawn from comparison between in-situ point measurements and soil moisture predictions from satellite data. Nonetheless, the following comparison is made to illustrate these issues.

In-situ point measurements of 0-5 cm deep gravimetric soil moisture were made at three locations i.e. Little Washita (LW), El Reno (ER) and Central Facility (CF). The relative locations of these sites are shown in Figure 7. At each of the locations, several fields were selected, and within each field, several measurements of soil moisture were made almost daily for about a month. Efforts were made to collect daily soil moisture samples in the same general vicinity to facilitate temporal comparisons of soil moisture. A specific pattern to walk in and out of the fields was followed.

Figure 8 shows the measured soil moisture spatial variability for LW on the four days. It is noticed that there is a definite pattern in spatial variability of soil moisture that repeats itself for all the four days. This variability could be the result of soil properties of the area. A similar variability pattern is also noticed in the soil moisture data from other locations at ER and CF. The plots showing spatial variability at ER and CF are not given here.

Despite spatial variability at LW, ER and CF, the soil moisture measurements from all samples for a particular location on a given day are averaged and the results are plotted in Figure 9(a). Except for CF on June 29, soil moisture decreases from June 29 to July 2. It is also noticed that soil moisture in the northern location (i.e. CF and ER) is higher than soil moisture in the southern location i.e. at LW.

To compare these in-situ averaged soil moisture with the soil moisture retrieved from satellite data, the soil moisture estimates from 1-km resolution are averaged over a 5km x 5km grid area for each of the LW, ER and CF locations. The 5km x 5km area could contain roads and buildings and thus the pixels in these areas do not correspond to the data points used in the in-situ measurements. Figure 9(b) shows a plot of volumetric, 1-km resolution soil moisture predictions for the four days at the three locations. A comparison of figures 9(a) and 9(b) shows that the temporal trend in the predicted soil moisture agrees with the generally decreasing soil moisture trend in the measurements. Also, a lower soil moisture value at the southernmost location (LW) is in agreement with the measurements. It should be mentioned here that the predicted soil moisture is for skin layer only and therefore, comparison of its magnitude with in-situ measurements is not warranted.

IV.   ERROR ANALYSIS AND SENSITIVITY STUDY

Since a firm comparison between the in-situ soil moisture and satellite-derived soil moisture is difficult to make, an estimate of different kinds of errors in the proposed

retrieval processes has been done to help understand the error budget. The total error is broken down into respective errors in the low-resolution (microwave) and high-resolution (optical/IR) parts of the algorithm. Errors from each of these parts have been further subdivided to the next level for simplifying the error budget calculation. Appendix B provides the definitions of accuracy, precision and uncertainty used in the error budget calculations.

A. *Error in Soil Moisture Estimation at the Microwave Resolution*

Total error in the microwave estimation of soil moisture is composed of two separate errors. The first error is the microwave algorithm error and is due to the inversion procedure employed to retrieve soil moisture from the microwave data. The second error is contributed by the data accuracy and precision.

(i) Microwave Algorithm Error (E_{m1}): As described in Section IIIA, a radiative transfer model has been used to invert dual-polarized microwave brightness temperature. To estimate error in this procedure, we have generated microwave brightness temperature data for four different types of land surfaces using Peake's modeling approach (Peake, 1959). The emission model incorporates a discrete scatter model and a Kirchhoff's model for vegetation and rough surface, respectively. It has been used extensively in the forward modeling of agricultural crops (Chauhan et al., 1994), grassland (Saatchi et al., 1994) and forest canopies (Chauhan et al., 1999). A brief description of the emission model is given in the Appendix A. This model is used to generate different surface types such as: bare and smooth, bare with low roughness (s=1 cm and l=10 cm), bare and rough (s=3 cm and l=10 cm), and vegetated (Leaf Area Index, LAI=3). In above, s denotes the RMS surface height of the rough surface and l is the correlation length of the surface. For vegetated terrain, the canopy parameters from a typical soybean field are used for the modeling (Table I). The leaf dimensions and density of the soybean canopy are equivalent to a canopy of LAI=3. The forward model results are inverted using the dual polarization technique described earlier. Figure 10 shows the retrieved results for the four types of terrain. The RMS errors in the soil moisture estimation are 3.6, 3.7, 0.5 percent for vegetated, bare rough and bare low-roughness terrain, respectively. The RMS error for the smooth bare surface is negligibly small. The estimation has been carried out for the soil moisture range of 0 - 35 percent.

(ii) Error Due to Data Accuracy and Precision (E_{m2}): For the purpose of the analysis, it is assumed that the accuracy and precision in temperature (LST as well as brightness temperature) are 1K and 0.5K, respectively (NPOESS, 1999). To calculate error in the soil moisture estimation due to data accuracies, temperatures are biased by $\pm$ 1K. Similarly, to calculate errors due to data precision, temperatures are perturbed by 0.5K around their mean values. These new temperatures are then used in the microwave algorithm to estimate soil moisture. It is found that the root mean square error in soil moisture estimates because of above accuracy and precision margin is on the order of 1-2 percent. This was expected because soil moisture in the dual-polarized algorithm depends on (T-Th)/(T-Tv). Because of ratioing, the effect of accuracy and precision of temperature on soil moisture is minimal. Similar analysis was also carried out in details in Chauhan (2001).

11

B. Error in Soil Moisture Estimation at High Resolution

There are again two sources of errors in the soil moisture estimation at high resolution (Section IIIB); first is the regression error (E_{v1}), and the second is precision error (E_{v2}) due to NDVI, LST and Albedo. To estimate E_{v1}, a system of linear equations (Equation 10) is set up using SSM/I-derived soil moisture, aggregated NDVI, albedo, and LST for the scene area. The system is solved, and regression coefficients for the second order polynomial fit are determined. The regression coefficients, and aggregated optical/IR parameters (NDVI, albedo, and LST) are used in the right-hand side of Eq. (10) to obtain 25-km resolution soil moisture values for the scene. The regression error is computed as the RMS error between the microwave soil moisture using a regression coefficient and a previous direct estimate of soil moisture from the SSM/I data. For this particular scene, the regression error (E_{v1}) is calculated to be 1.6 percent. Analysis performed on other scenes also produced the same order of regression error (Chauhan et al., 1998). The relatively lower value of regression error indicates that there are enough training data points in regression and the regression coefficients are reasonable.

To compute E_{v2}, we flowed down precision error in LST, NDVI, and albedo in the high-resolution soil moisture algorithm. We have assumed precision (P) in LST, albedo, NDVI as 0.5K, 0.020, 0.02, respectively. These precision numbers are taken directly from the Sensor Requirement Document of NPOESS (NPOESS, 1999). One-by-one, the three inputs are perturbed randomly around their mean value by ± P. The soil moisture resulting from perturbed input to Eq. (10) are compared to that obtained from the unperturbed inputs. The root mean square error (E_{v2}) due to precision error in LST, albedo and NDVI are computed to be 0.338, 0.722 and 1.57 percent, respectively.

An examination of Eq. (10) reveals that the microwave-derived soil moisture M is related to the scene variations in NDVI, albedo and LST and not to their absolute values. The parameters NDVI*, A*, and T* in Eqs. (6), (7), and (10) define these relative variations. Therefore, accuracy errors (or bias) of NDVI, LST and albedo is likely to have little effect on the high-resolution soil moisture estimation. Consequently, we have not calculated the effect of accuracy errors in LST, NDVI and albedo on the soil moisture estimation procedure for high resolution.

Assuming that the errors are uncorrelated, the total error budget for soil moisture can now be given as $\sqrt{E_{m1}^2 + E_{m2}^2 + E_{v1}^2 + E_{v2}^2}$. Based on the above error budget calculations, the total error in soil moisture estimation (final product) using the current technique is less than 5 percent. For bare smooth surface, the error is lesser. This error is well within the requirements set by NPOESS for the soil moisture estimation. Note that all but the microwave algorithm errors are computed for the satellite data. A summary of all the errors is given in Table II. Clearly, the algorithm error is the largest error source. In the present case, this error is estimated from simulated data and can go higher for real data from satellites.

12

VI. DISCUSSION

The aforementioned process for high-resolution soil moisture determination involves a synergistic analysis of microwave-optical/IR data. The algorithm combines the traditional accuracy of microwave sensors for soil moisture sensing with the high-resolution capability of optical/IR sensors to determine soil moisture estimates at high-resolution. An important component of the operational retrieval process for operational use is the use of dual-polarization microwave data for obtaining surface reflectivity, which is later converted to soil moisture. The dual-polarization technique used here is a departure from single polarization techniques that have been used for most of the past soil moisture estimation work. The technique is suitable for global soil moisture estimation from satellite data because it does not require 'a priori' information about vegetation and surface roughness condition. Since SSM/I frequency (19.4 GHz) can not penetrate all vegetated surfaces, NDVI values are used to limit the application of the dual polarization algorithm to the weakly vegetated pixels.

Vegetation has been assumed as an absorbing medium only and the scattering from vegetation is ignored. Incoherent scattering from the rough surfaces is also not accounted for in the inversion process. Most of the studies involving soil moisture estimation from large scale experiments, such as MACHYDRO-90, Washita-92, Washita-94, SGP-97, etc., have made similar assumptions and found reasonable agreement with in-situ soil moisture data. The proposed dual polarization method for the microwave soil moisture is expected to be an improvement over the previous techniques because incoherent scattering effects are minimized in the ratioing process.

The signals from SSM/I and AVHRR may not be sensing soil moisture to the same vertical depth. As a result, their soil moisture estimates can differ. Microwave radiometers measure soil moisture in the topmost soil layer. At 19 GHz, this layer can be less than half a centimeter deep. Strictly speaking, the 'universal triangle' method relates soil moisture availability (ratio of soil water content to field capacity) to radiant temperature and fractional vegetation cover ($\sim NDVI*^2$). It is possible that the estimates of soil moisture using the above two methods are different. But in the approach outlined here, the 'universal triangle' concept is used to establish relations between soil moisture, temperature, albedo, and NDVI. This should have a minimal effect on the process of disaggregation employed here to enhance spatial resolution of the soil moisture.

The technique described here to link low-resolution soil moisture with the land parameters has a definite theoretical basis in the surface energy balance technique. The 'universal triangle' is the result of numerous simulations carried out using the soil vegetation atmosphere transfer modeling. The simulations have also been validated using data from different field experiments (Gillies et al. 1997). The SVAT simulations requires micrometeorological and other data and early simulations were conducted using data collected at a field campaign in Mahantango, during MACHYDRO-90 experiment. For the remote sensing applications it was found that that a regression relation like equation (8) gives results similar to those obtained by SVAT model (http://www.essc.psu.edu/~tnc). Sensitivity tests have shown that the distribution of

13

isopleths inside the triangle is insensitive to the initial conditions and so one can get by using a single polynomial to represent a wide range of surface climate conditions and land surface types (Carlson, 1998).

The regression error can vary from scene to scene and also depends on the size of the scene. In addition, if the training area (where regression coefficients are derived) and the test area (where regression is applied) are the same, the regression error is small. For the NPOESS soil moisture, it is proposed to determine separate regression coefficients for each contiguous scene in the orbit. This will ensure reduced regression error. In cases, where the swath widths of VIIRS and CMIS do not overlap, the regression coefficients from adjacent scene will be used and as a result, the error in soil moisture estimation will be higher.

Eq. (9) represents nth order polynomial fit between the microwave-derived soil moisture, NDVI, LST, and albedo. We performed a sensitivity analysis on the order of polynomial used in the regression by using a lower and a higher-order polynomial in Eq. (9). A third order polynomial with seventeen terms was found to be more accurate but less flexible to extrapolate soil moisture values outside the range for which the regression coefficients are derived. On the other hand, a first order polynomial with four terms was less accurate, but it could extrapolate soil moisture values over a wider soil moisture range. We conclude that a second order polynomial is a reasonable fit in Eq. (9).

APPENDIX A
MICROWAVE EMISSION MODEL FOR LAND

Microwave radiometer response is obtained by summing up all the energy over the hemisphere above the canopy (Fig. A1). We have followed Peake's approach (1959) that assumes thermal equilibrium so that energy absorbed is equal to the energy emitted. The emitted energy or emissivity is expressed as one minus the scattering albedo (Ulaby et al., 1982), and therefore, the microwave brightness temperature T_q ($q \in h,v$) can be expressed as

$$T_q = (1 - W_q)T \tag{A1}$$

where T is physical temperature of the scene, W_q is the scattering albedo and is made up of specular and diffused components i.e. $W_q = W_q^{diff} + W_q^{spec}$, where W_q^{diff} and W_q^{spec} are diffused and specular albedos respectively (Fig. A1). These albedos are scene albedos and are different from the single scattering albedo. The specular albedo for a vegetated rough surface is given as

$$W_q^{spec} = \Gamma_{sq} \Gamma_{iq}^* e^{-2\tau_q} e^{-4k_o^2 s^2 \cos^2 \theta_i} \tag{A2}$$

where Γ_{iq} and Γ_{sq} are the Fresnel reflection coefficients of the flat surface in the incident and the scattered (specular) direction respectively. The asterisk (*) over Γ_{iq} denotes its complex conjugate. Earlier in Section IIIA we used R_h and R_v to denote the reflection coefficients which is real part of Γ_{iq}. The diffused albedo from a vegetated rough surface is contributed both by the vegetation and the rough surface. It can be expressed as sum of the vegetation and rough surface albedos. Mathematically, either one of the latter can be obtained by integrating the scattering coefficients over the hemisphere above the scene as (Chauhan et al., 1994)

$$W_q^{diff} = \frac{1}{4\pi \cos \theta_i} \int \left[\sigma_{hq}^o(\mathbf{o},\mathbf{i}) + \sigma_{vq}^o(\mathbf{o},\mathbf{i}) \right] d\Omega_s \tag{A3}$$

where $\sigma^o(\mathbf{o},\mathbf{i})$ are bistatic scattering coefficients of the vegetation or the rough surface. These are calculated using distorted Born approximation (Lang and Sidhu, 1983) and Kirchhoff's rough surface approach (Ulaby et al., 1982) for the vegetation and rough surface, respectively. The integration is carried over the upper hemisphere where $d\Omega_s = \sin \theta_s d\theta_s d\varphi_s$. Assuming that the scattering from the rough surface and vegetation canopy are independent, Eq. (A1) can be rewritten as

$$T_q = \left\{ 1 - (W_q^{spec} + W_{q,s}^{diff} + W_{q,v}^{diff}) \right\} T \tag{A4}$$

15

where $W_{q,s}{}^{diff}$ and $W_{q,v}{}^{diff}$ denotes diffused albedos from the surface and vegetation respectively. More details about the emission model can be found in Chauhan et al. (1994).

The above model gives excellent results and has been validated for a variety of land covers such as corn, grass and forest (Chauhan et al., 1994; Saatchi et al., 1994; Chauhan et al., 1999). The model is difficult to invert due to the presence of diffused scattering terms from rough surface and vegetation. However, the model can be simplified and made invertible if the diffused albedo W^{diff} due to surface as well as due to vegetation, can be assumed negligibly small. This condition can be satisfied if the terrain is lightly vegetated and/or have low surface roughness conditions. Therefore, equation (A1) is simplified as

$$T_q = T(1 - \left|R_g^q\right|^2 e^{-2\tau_q} e^{-4k_a^2 s^2 \cos^2 \theta_i})$$
(A5)

Above equation is identical to Equation (3) given earlier in Section IIIA. In the above equation $\left|R_g^q\right|^2 = \Gamma_{sq}\Gamma_{iq}^*$.

It is assumed in (A1) that the atmospheric and sky contributions to T_q are small and are negligibly small. Microwave brightness temperatures from space are modified by atmosphere. Short-term comparisons of T_B are generally valid at low frequencies; however, over longer periods (seasonal or yearly) it is necessary to take atmosphere into account. As noted by Choudhury (1993), the magnitude of the effect of atmosphere at mid-latitudes at 19 GHz can of the order of +3K. CMIS frequency used for the soil moisture retrieval process for NPOESS is likely to be lower than 19 GHz. As a result, atmospheric contribution to brightness temperature will be negligibly small.

APPENDIX B
ACCURACY, PRECISION AND UNCERTAINTY

We have followed the following definitions given in the NPOESS (1999) document. Accordingly, the measurement accuracy A is defined as

$$A = |\mu - T|$$

(B1)

where

$$\mu = \frac{1}{N} \sum_{i=1}^{N} X_i$$

(B2)

and μ is the average of all the measured values X_i corresponding to a true value T. The precision P, as defined in NPOESS (1999), is the standard deviation of the measurements from their average value and is expressed as

$$P = \sqrt{\frac{1}{N-1} \sum_{i=1}^{N} (X_i - \mu)^2}$$

(B3)

Finally, the uncertainty is defined as

$$U = \sqrt{\frac{1}{N} \sum_{i=1}^{N} (X_i - T)^2}$$

(B4)

From the above definition, one can write

$$U = \sqrt{A^2 + P^2}$$

(B5)

Thus, the uncertainty equals the RMS error between the measurements X_i and the true value T. It is important to note here that precision and accuracy are quite different yardsticks for characterizing data quality.

REFERENCES

Beljaars, A., P. Viterbo, M. Miller and A. Betts (1996). The anomalous rainfall over the United States during July 1993: Sensitivity to land surface parameterization and soil moisture anomalies. Mon. Weath. Rev., vol. 124, pp. 362-383.

Brubaker, L., and D. Entekhabi (1996). Analysis of feedback mechanisms in land-atmosphere interaction. Water Resour. Res., vol. 32, pp. 1343-1357.

Carlson, T., R. Gillies, and E. Perry (1994). A method to make use of thermal infrared temperature and NDVI measurements to infer surface soil water content and fractional vegetation cover. Remote Sensing Reviews, vol. 9, pp. 161-173.

Carlson, T., R. Gillies, T. Schmugge (1995). An interpretation of methodologies for indirect measurements of soil water contents. Agricul. and Forest Meteor., vol. 77, pp. 191-205.

Carlson, T. (1998). Personal Communication.

Chauhan, N., D. LeVine, and R. Lang (1994). Discrete scatter model for radar and radiometer response to corn: comparison of theory and data. IEEE Trans. Geosc. & Remote Sens., vol. 32, pp. 416-426,1994.

Chauhan, N. (1997). Soil moisture estimation under a vegetation cover: combined active passive remote sensing approach. Int. J. Remote Sens., vol. 18, pp. 1079-1097.

Chauhan, N., L. Di, S. Miller and P. Ardanuy (1998). Soil moisture visible/infrared imager/radiometer suite Algorithm Theoretical Basis Document - Version I. SRBS Document # Y2387, Raytheon, Lanham MD 20706.

Chauhan, N., D. LeVine and R. Lang (1999). Passive and active remote sensing of soil moisture under a forest canopy. International Geoscience and Remote Sensing Symposium Proceedings, pp. 1914-1916, Hamburg, Germany.

Chauhan, N. (2001). Soil moisture inversion at L-band using dual polarization technique: A model based sensitive analysis (in press). Int. J. Remote Sensing.

Choudhury, B. (1993). Reflectivities of selected land surface types at 19 and 37 GHz from SSM/I observations. Remote Sens. Environ., vol. 46, pp. 1-17.

Cracknell, A., and Y. Xue (1996). Thermal inertia determination from space – a tutorial review. Int. J. Remote Sens., vol. 17, pp. 431-461.

Delworth, T., and S. Manabe (1989). The influence of soil wetness on near surface atmospheric variability. J. Clim., vol. 2, pp. 1447-1462.

England, A., J. Galantowicz, and M. Schretter (1992). The radiobrightness thermal inertia measure of soil moisture. IEEE Trans. Geosci. and Remote Sens., vol. 30, pp. 132-139.

Engman, T. (1991). Application of remote sensing of soil moisture for water resources and agriculture. Remote Sensing of Environ., vol. 35, pp. 213-226.

Gillies, R., T. Carlson, W. Kustas, and K. Humes (1997). A verification of the "triangle" method for obtaining surface soil water content and energy fluxes from remote measurements of the Normalized Difference Vegetation Index (NDVI) and surface radiant temperature. Int. J. Remote Sens., vol. 18, pp. 3145-3166.

Hallikainen, M., F. Ulaby, M. Dobson, and M. El-Rayes (1985). dielectric behavior of wet soil-Part I: Empirical models and experimental observations. IEEE Transactions on Geosci. and Remote Sens., vol. 23, pp. 25-34.

Idso B., T. Schmugge, R. Jackson, and R. Reginto (1975). The utility of surface temperature measurements for remote sensing of soil water studies. J. Geophys. Res., vol. 80, 3044-3049.

Idso, S., R. Jackson, and R. Reginato (1976). Compensating for environmental variability in the thermal inertia approach to remote sensing of soil moisture. J. of Applied Meteor., vol. 15, pp. 811-817.

Jackson, T., T. Schmugge, and J. Wang (1982). Passive sensing of soil moisture under vegetation canopies. Water Resources Research, vol. 18, pp. 1137-1142.

Jackson, T. (1997). Soil Moisture estimation using special satellite microwave/imager satellite data over a grassland region. Water Res., vol. 33, pp. 1475-1484.

Lang, R. and J. Sidhu (1983). Electromagnetic backscattering from a layer of vegetation: A discrete scatter approach. IEEE Transactions on Geosci. and Remote Sens., vol. 21, pp. 62-71.

Myneni, R., R. Nemani, and S. Running (1997). Estimation of global leaf area index and absorbed PAR using radiative transfer models. IEEE Trans. Geosc. & Remote Sens., vol. 35, pp. 1380-1393.

Nemani, R., S. Running, L. Pierce, and S. Goward (1993). Developing satellite derived estimates of surface moisture status. Journal of Applied Meteorology, vol. 32, pp. 548-557.

Njoku, E. and L. Li (1999). Retrieval of land surface parameters using passive microwave measurements at 6-18 GHz. IEEE Transactions on Geosci. and Remote Sens., vol. 37, pp. 79-93.

NPOESS, (1999). Sensor Requirements Document, Integrated Program Office, Silver Spring, MD 20910.

O'Neill, P., N. Chauhan, T., and Jackson (1996). Use of active and passive remote sensing for soil moisture estimation through corn. Int. J. Remote Sens., vol. 17, pp. 1851-1865.

Owe, M., Van de Griend and A. Chang (1992). Surface moisture and satellite microwave observations in semiarid Southern Africa. Water Res., vol. 28, pp. 829-839.

Peake, W. (1959). Interaction of electromagnetic waves with some natural surfaces. IRE Trans. Antennas Propag., vol. AP-7, pp. S324-S329.

Price, J. (1977). Thermal inertia mapping: A new view of the Earth. J. Geophy. Res., vol. 82, pp. 2582-2590.

Price, J. (1984). Land surface temperature measurements from the split window channels of the NOAA-7/AVHRR. J. Geophy. Res., vol. 89, pp. 7231-7237.

Saatchi, S., D. LeVine and R. Lang (1994). Microwave backscattering and emission model for grass canopies. IEEE Transactions on Geosci. and Remote Sens., vol. 32, pp. 177-186.

Seller, P., Y. Mintz, Y. Sud and A. Dalcher (1986). A simple Biosphere model (SIB) for use within general circulation models. J. Geophy. Res., vol. 43, pp. 505-531.

Ulaby, F., M. Moore, and A. Fung (1982). remote sensing: Active and passive, vol. I-III. Reading, MA: Addison-Wesley Publishing Co.

Van de Griend, A., and M. Owe (1993). Determination of vegetation optical depth and single scattering albedo from large scale soil moisture and Nimbus/SMMR satellite observations. Int. J. Remote Sens., vol. 14, pp. 1875-1886.

TABLE 1.
SOYBEAN CANOPY PARAMETERS*

Canopy Parameters	Canopy height	60 cm
	Plant density	1000 /m**3
Leaf Parameters	Radius	4 cm
	Thickness	0.2 mm
	Density	1000 /m**3
	Dielectric Constant	25.3 +j7.96
	Inclination Angle	Uniform

*These parameters are derived from actual measurements carried out in a field experiment conducted at the Beltsville, MD USDA facility.

TABLE II
ERROR BUDGET FOR THE SOIL MOISTURE
ESTIMATION ALGORITHM (%)

Microwave Resolution:

Algorithm Error (E_{m1}):

Bare smooth	0.0005
Vegetated	3.6
Bare rough	3.7
Bare low rough	0.5

Accuracy & Precision error (E_{m2}) < 1

High Resolution:

Regression Error (E_{v1})   1.6

Precision Error (E_{v2}):

LST	0.338
NDVI	1.57
Albedo	0.722

FIGURE CAPTIONS

Figure 1. Schematic flow diagram for soil moisture estimation algorithm.

Figure 2. Universal Triangle - Schematic relationship between soil moisture temperature and *NDVI*.

Figure 3. Soil moisture map of the SGP-97 area estimated from SSM/I data (25-km resolution) for four days.

Figure 4. A plot of soil moisture for SSM/I pixels (25-km resolution) in the SGP-97 area for four days.

Figure 5. Soil moisture map at 1-km resolution of the SGP-97 area. There is a decreasing trend in soil moisture from June 29 to July 2. Note also that the northern area of the SGP-97 shows higher soil moisture compared to south.

Figure 6. A pixel value plot of soil moisture at 1-km resolution in the SGP-97 area for four days. Soil moisture range varies from 5-20 percent. One-to-one correspondence is observed between the data shown in figures 6 and 4 .

Figure 7. Location of three sites where in-situ soil moisture measurement were conducted during the SGP-97 experiment.

Figure 8. An example of spatial variability in 0-5 cm soil moisture in a particular field at Little Washita. The variability appears to be consistent for all the four days considered in the present study.

Figure 9. (a) An example of temporal and spatial variability in 0-5 cm soil moisture measured at the SGP-97 area. Point measurements from each location such as LW are averaged from the data collected from many fields in LW. LW and CF are located at south and north edge of the SGP-97 experimental area. (b) Retrieved surface soil moisture averaged over three locations for June 29-30, July 1-2, 1997. The averaging is done in a 5km x 5km area for a particular location. Note that the number and size of pixels averaged in (a) and (b) are not identical .

Figure 10. Microwave soil moisture inversion results for four different land surfaces. Dual polarization inversion is used.

Figure A1. Schematic representation of the emission model for vegetated terrain based on Peake's approach.
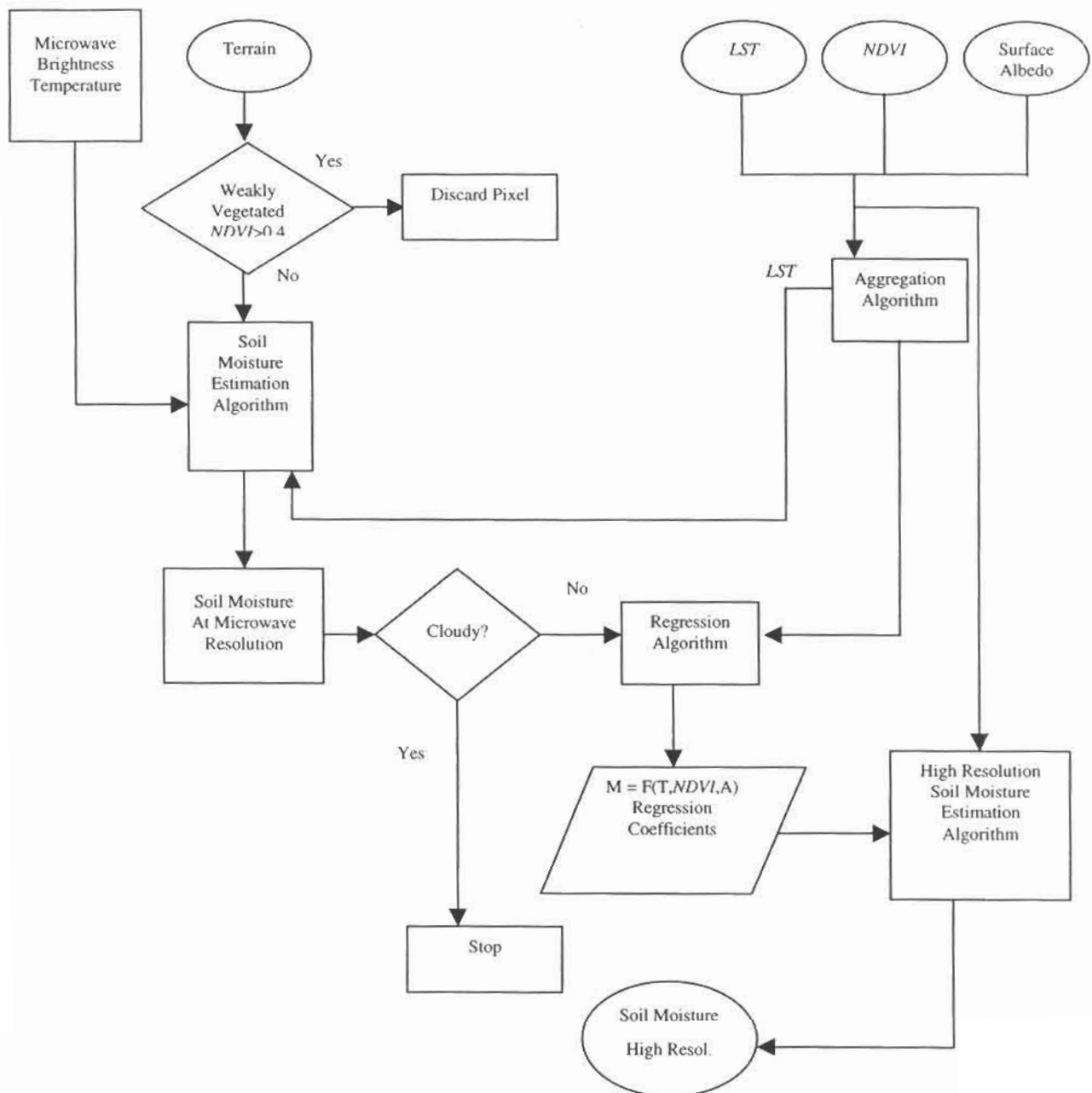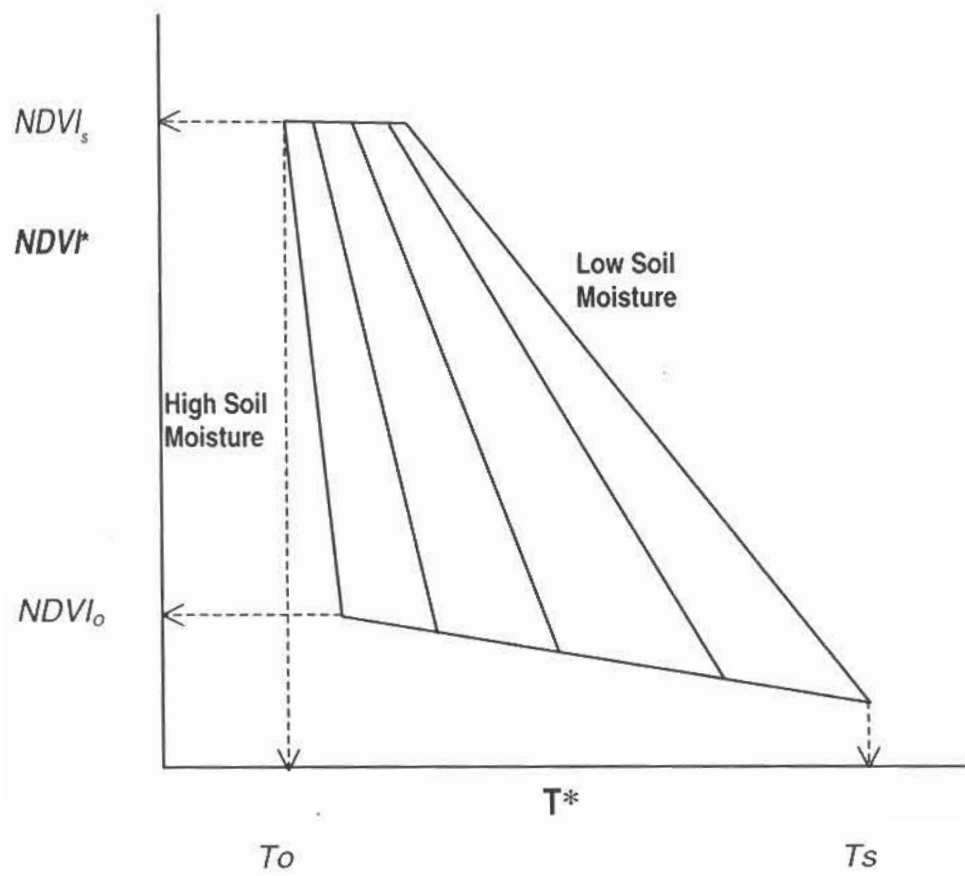
25 KM Microwave Soil Moisture on 06/29/97
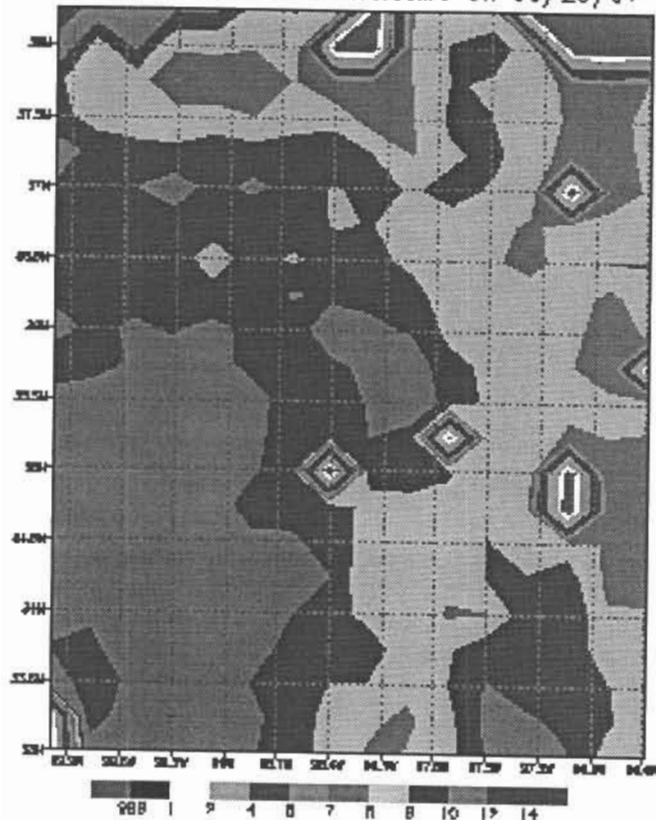
25 KM Microwave Soil Moisture on 06/30/97
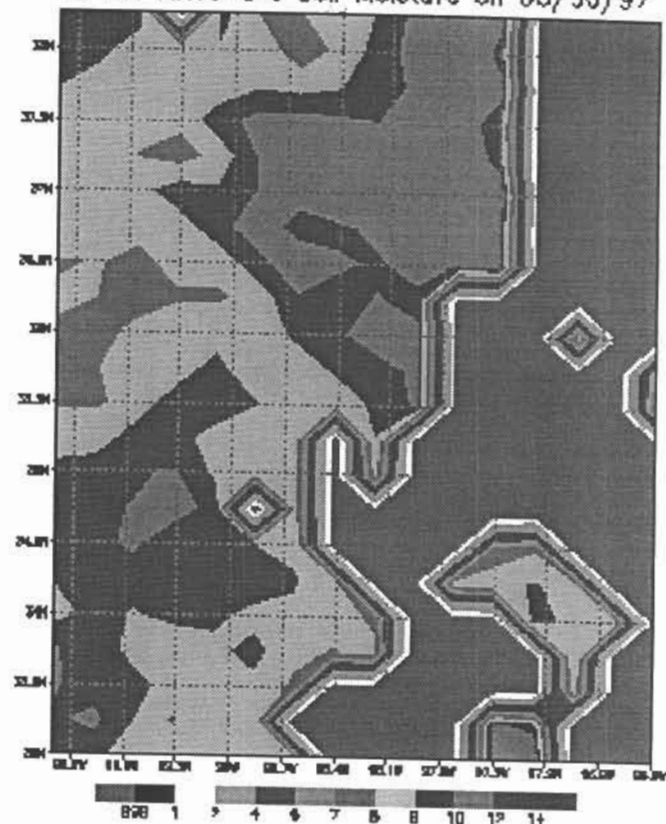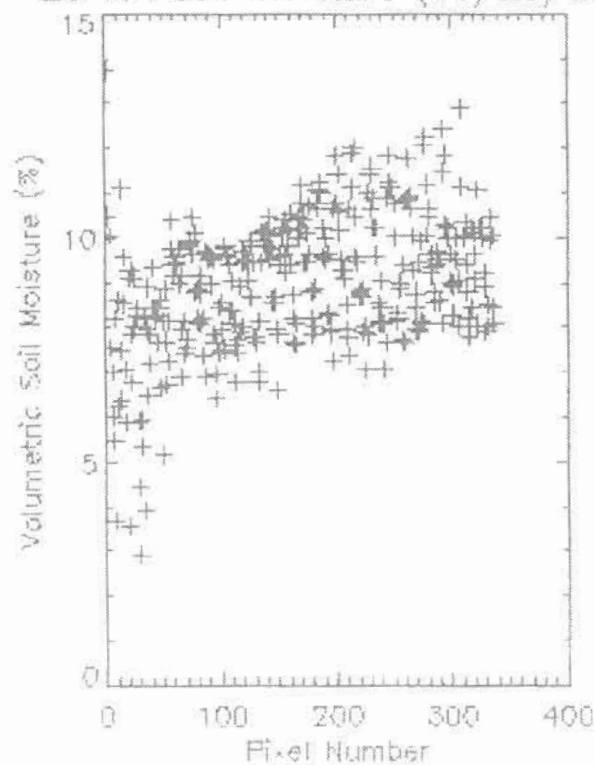
25 KM Microwave Soil Moisture on 07/01/97
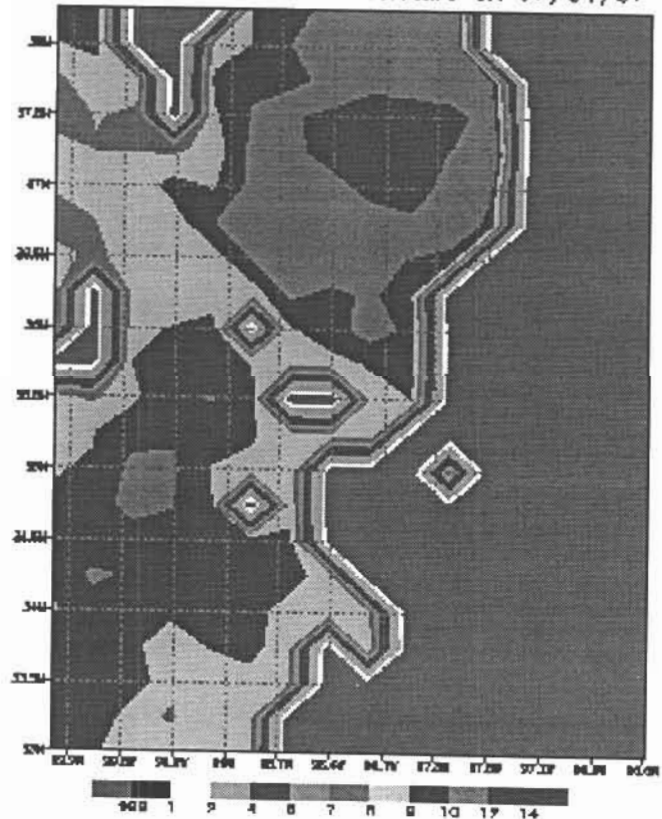
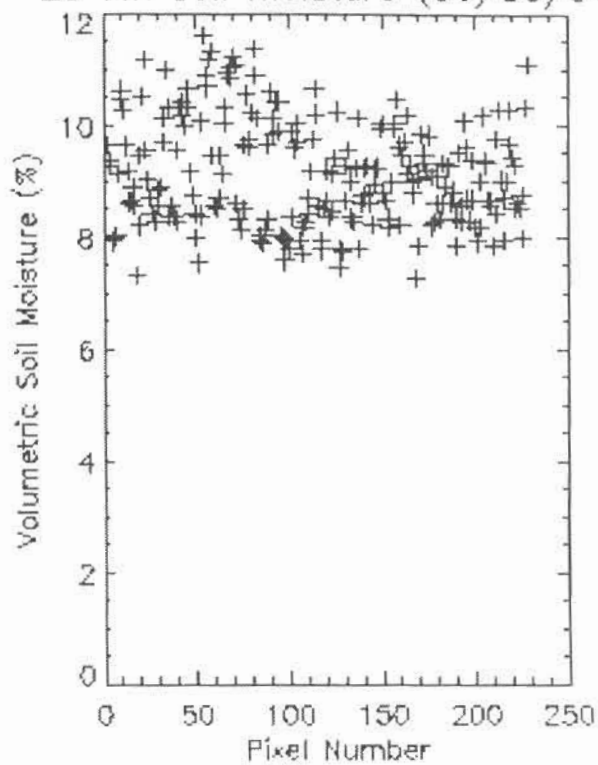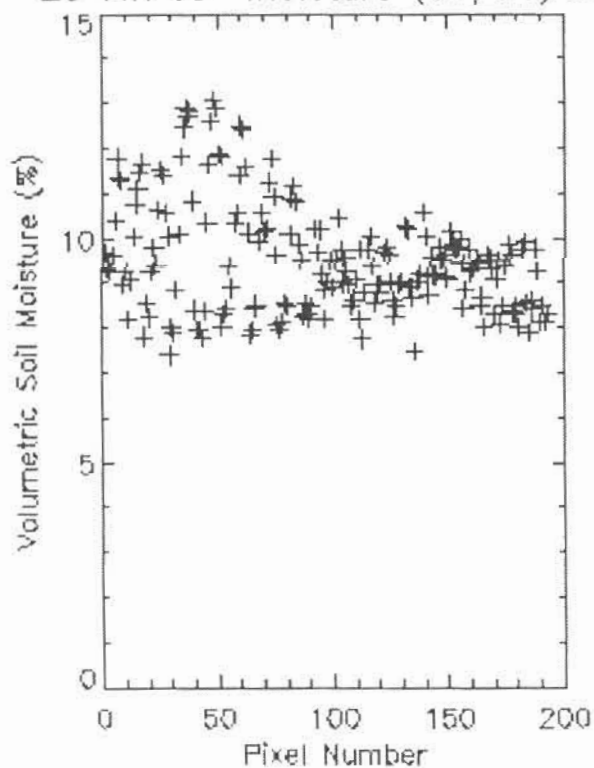25 KM Microwave Soil Moisture on 07/02/97
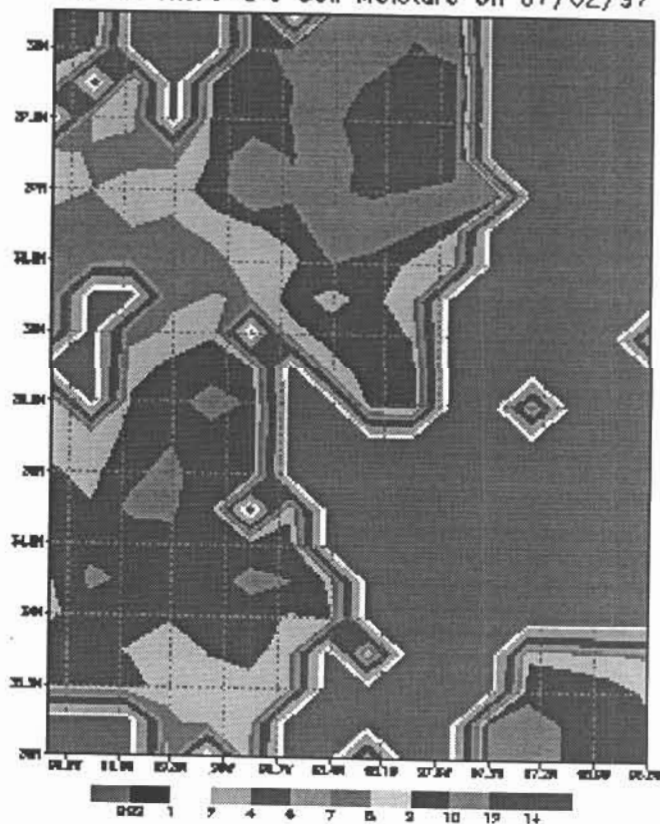
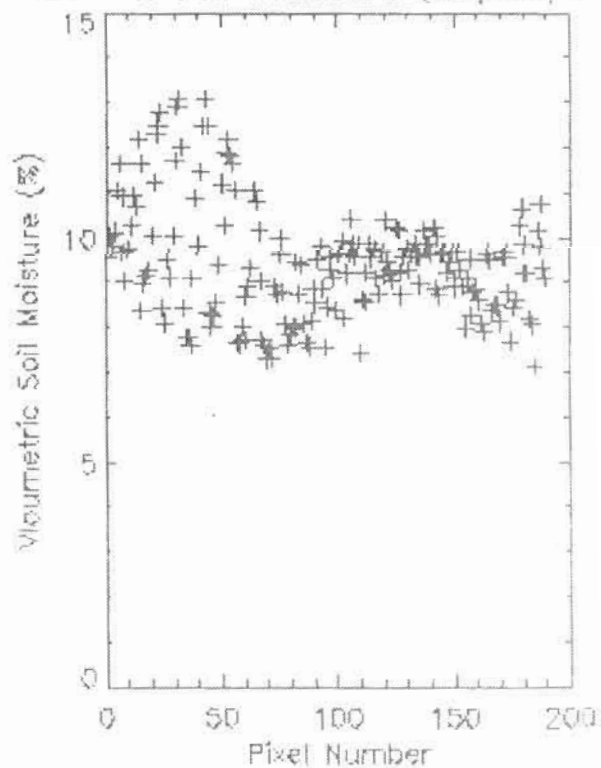25 km soil moisture (06/29/97)

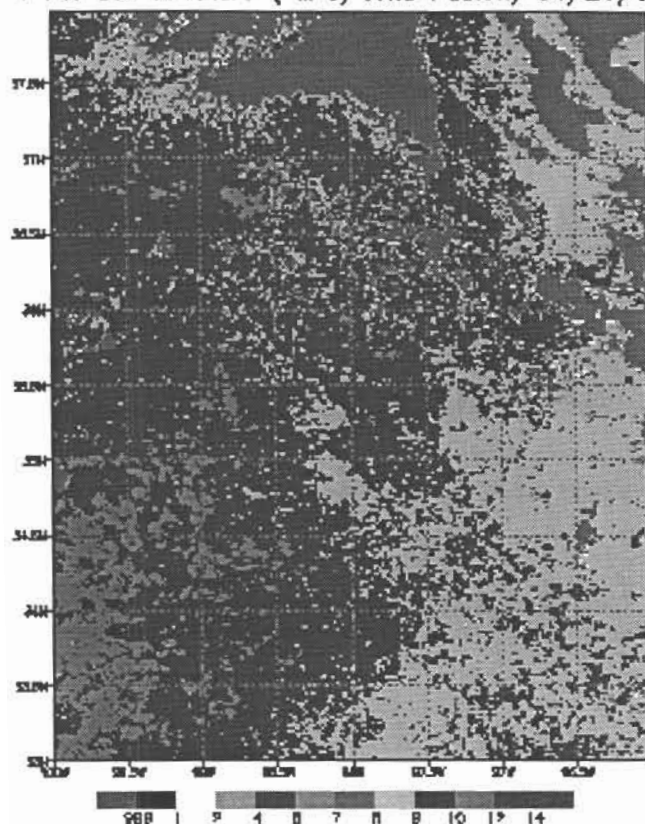25 km soil moisture (06/30/97)
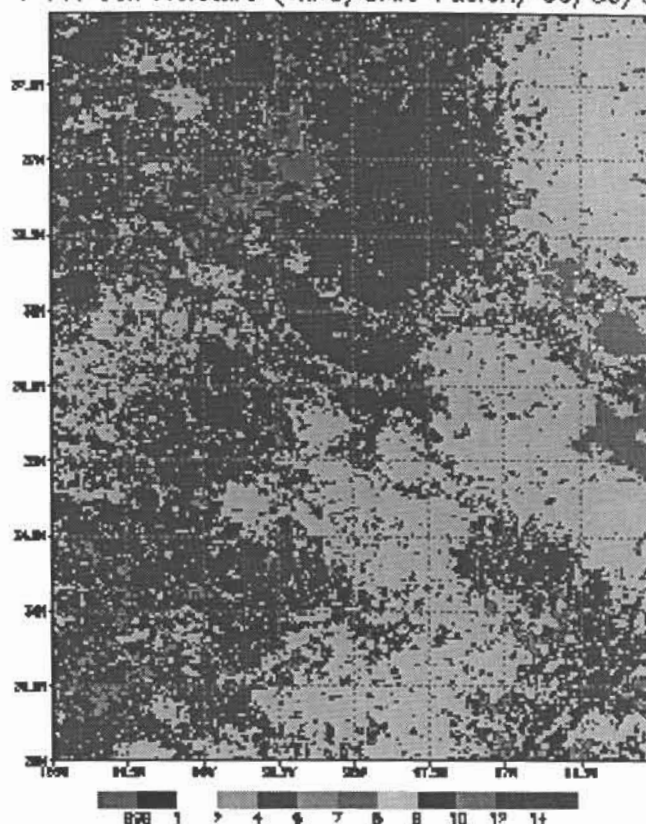
25 km soil moisture (07/01/97)
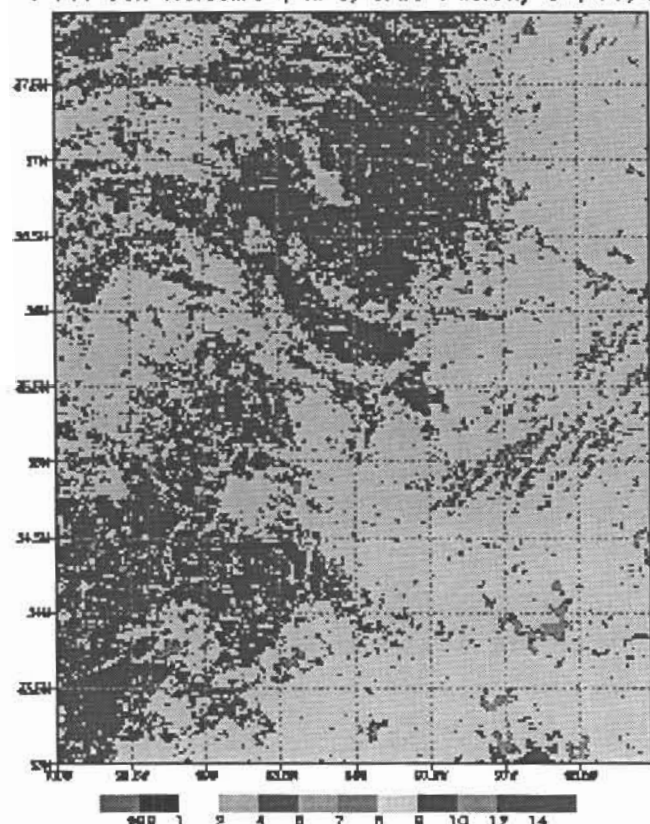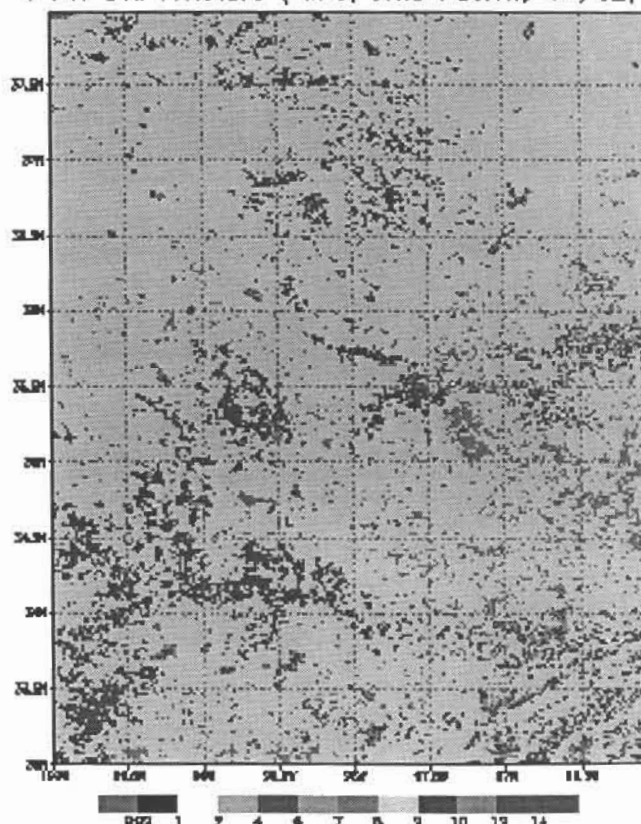
25 km soil moisture (07/02/97)

1 KM Soil Moisture (VIIRS/CMIS Fusion) 06/29/97
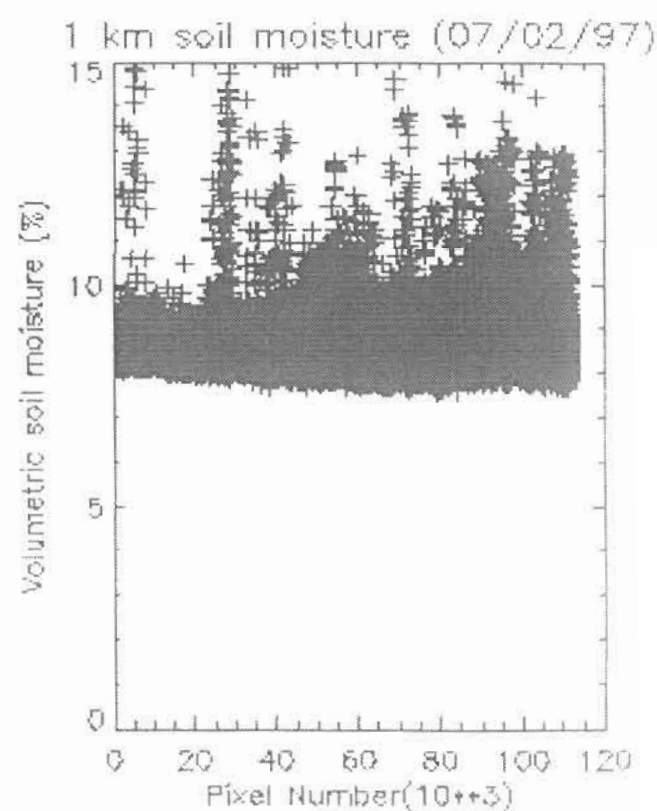
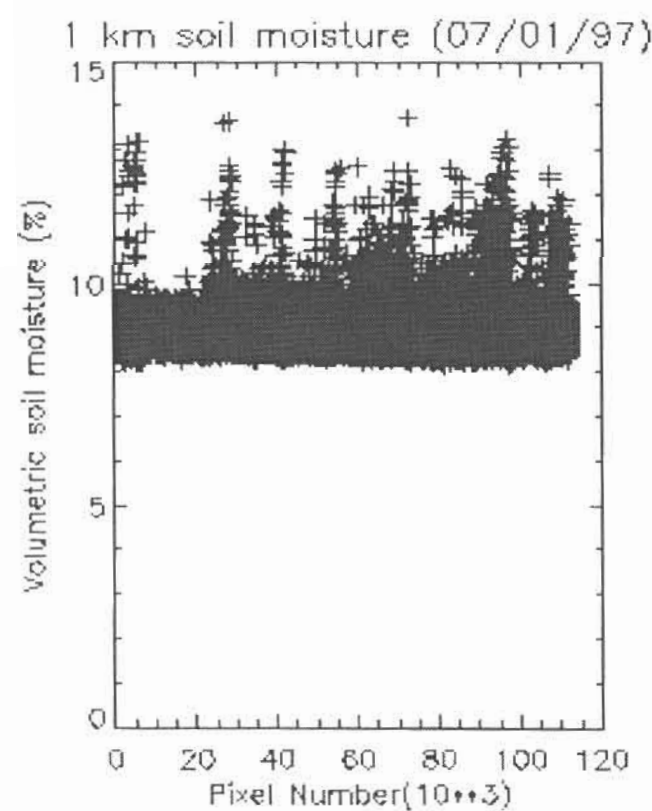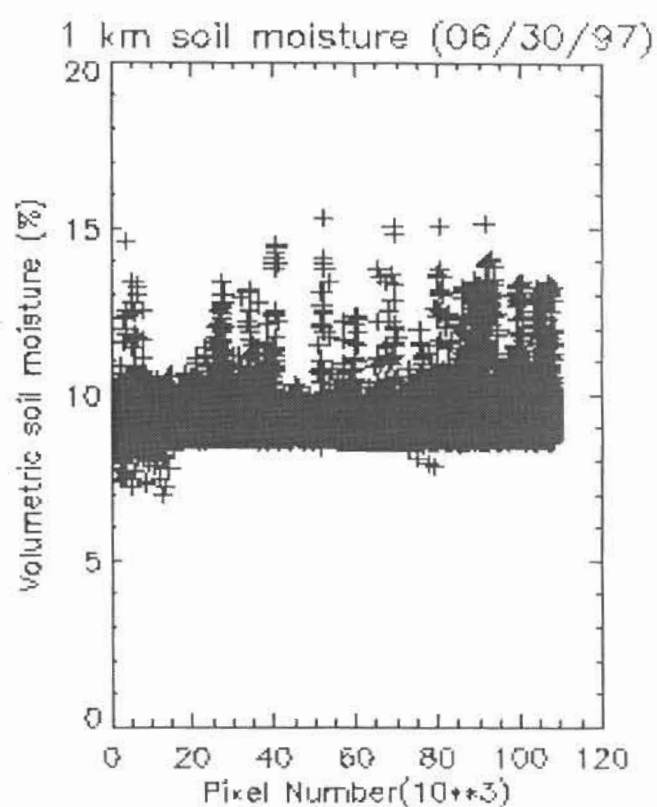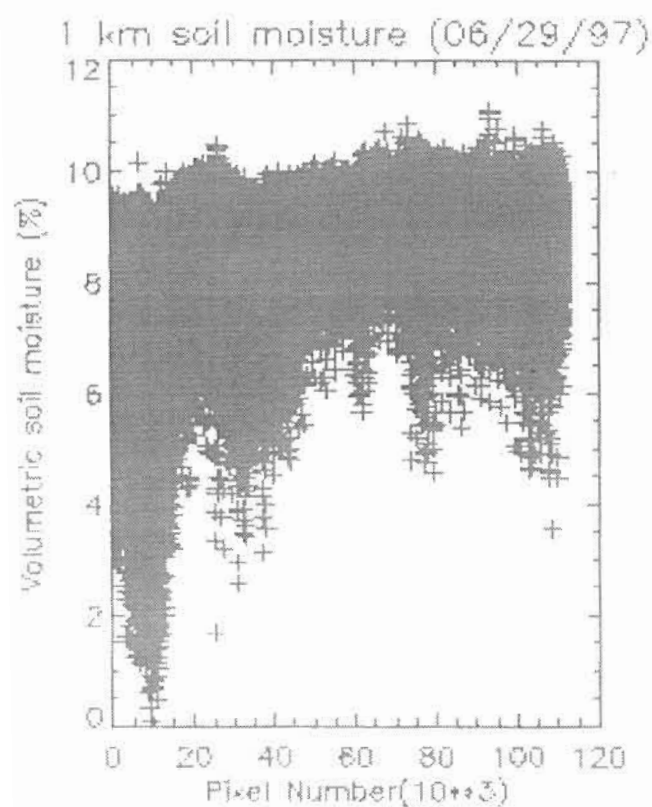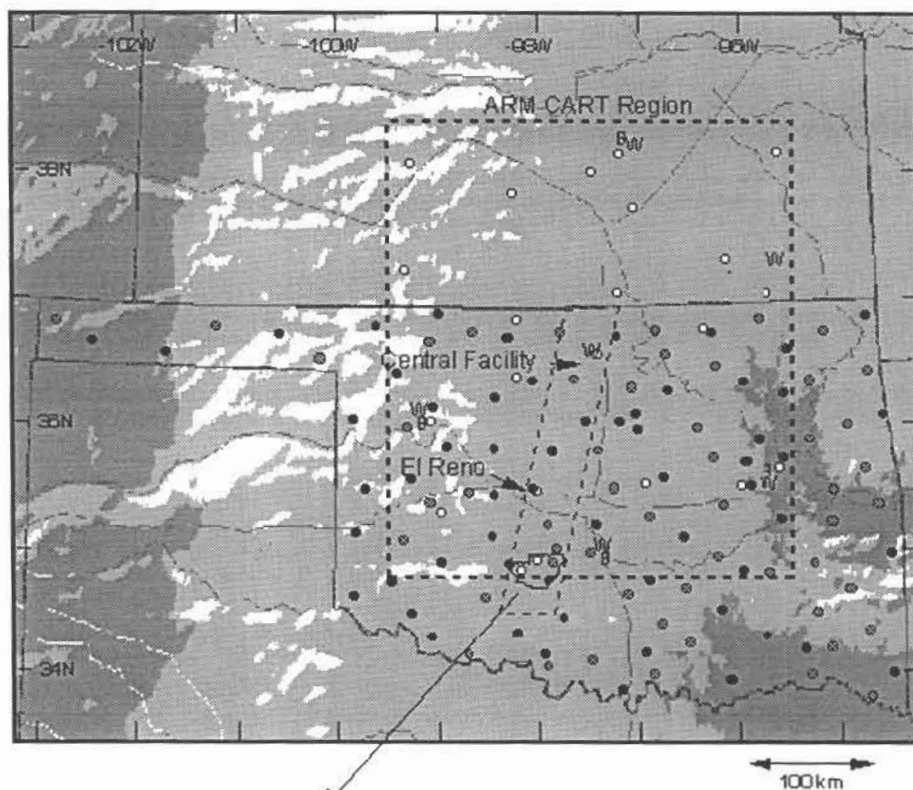1 KM Soil Moisture (VIIRS/CMIS Fusion) 06/30/97

1 KM Soil Moisture (VIIRS/CMIS Fusion) 07/01/97
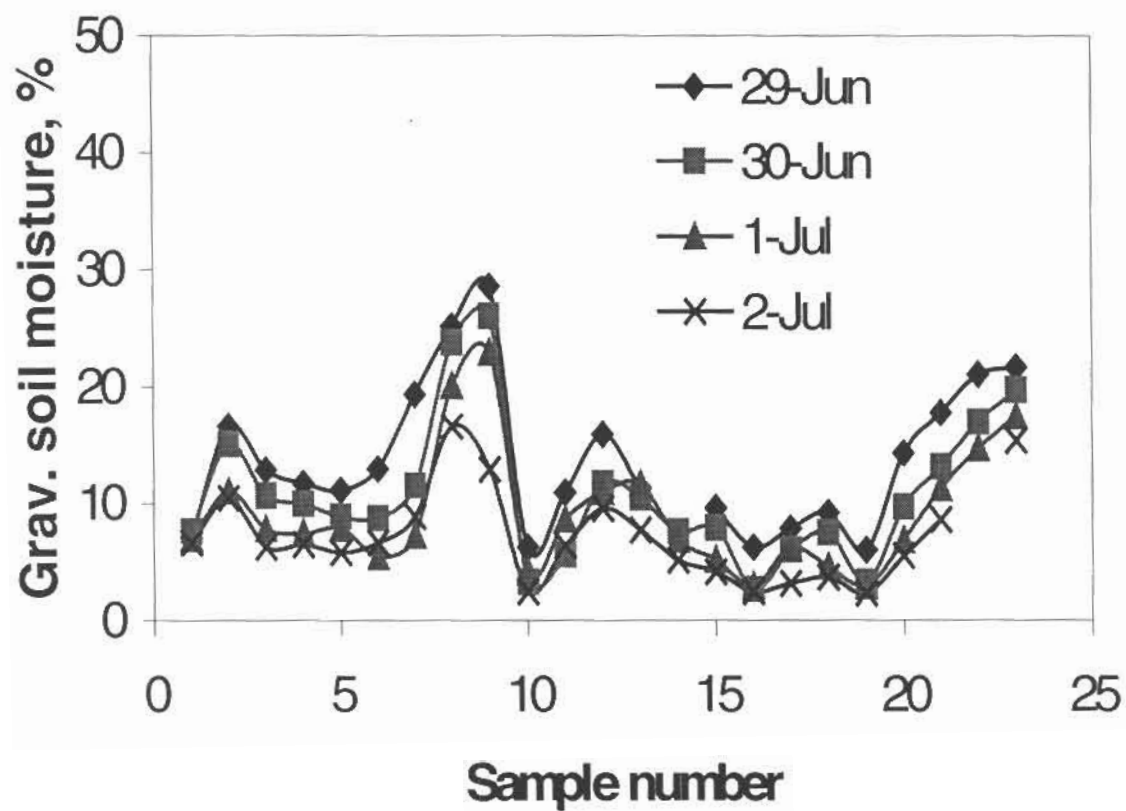
1 KM Soil Moisture (VIIRS/CMIS Fusion) 07/02/97

1 km soil moisture (06/29/97)

1 km soil moisture (06/30/97)
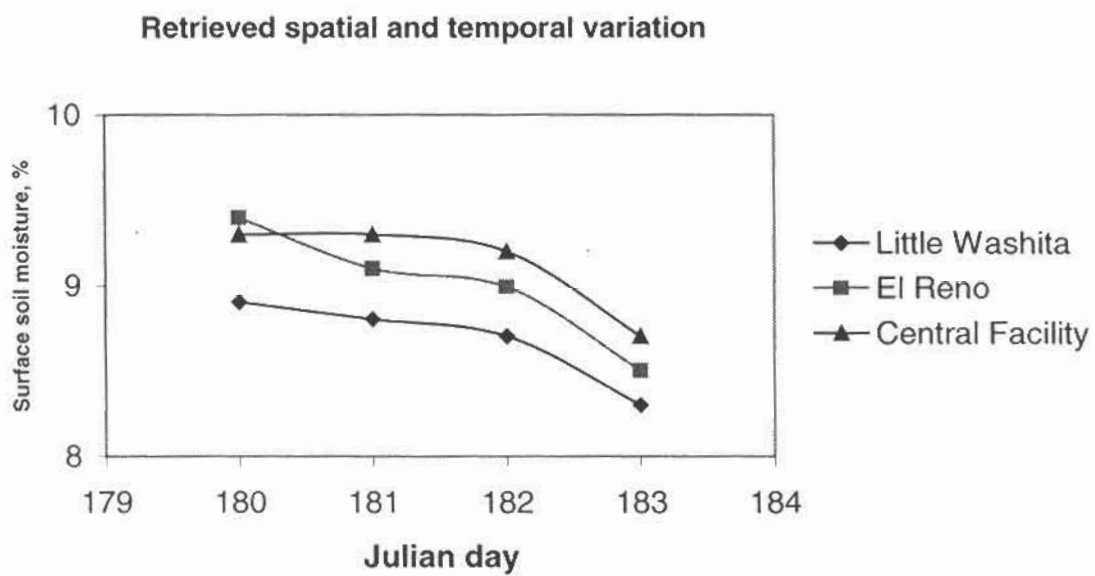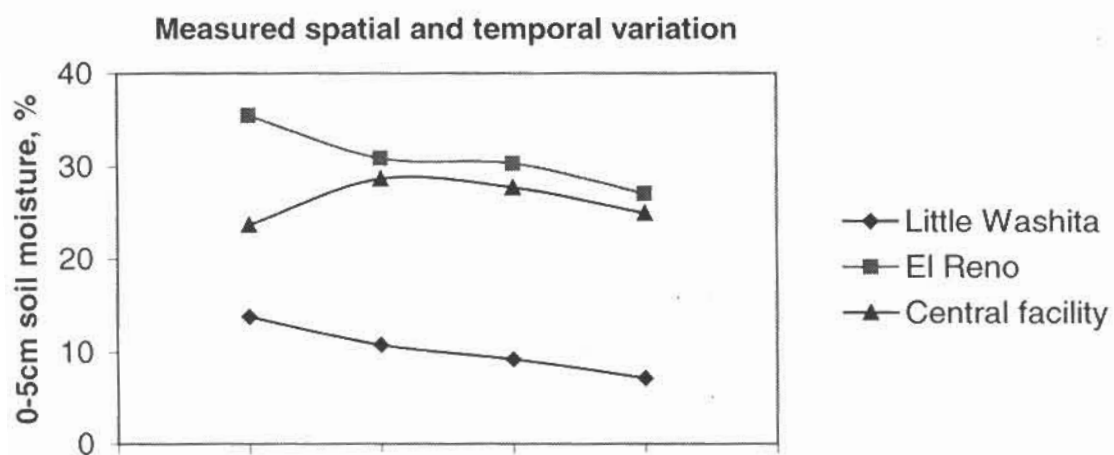
1 km soil moisture (07/01/97)

1 km soil moisture (07/02/97)

LITTLE WASHITA
WATERSHED

○ ARM CART
◆ Mesonet
● Mesonet with Soil Moisture
▲ Micronet with Soil Moisture
w ARM Wind Profiler
в ARM Boundary Facility

30

Spatial Variability at LW

Measured spatial and temporal variation

Retrieved spatial and temporal variation

Julian day

SM estimation - dual-pol.

Estimated soil moisture, %

- ◆ bare,smooth
- ■ vegetated, LAI=3
- ▲ bare, rough
- ✳ bare, low rough

True soil moisture, %

Incident

Diffused

Reflected (specular)

vegetation

ground